Aerosol Cloud Interaction and Raman Lidar, ACIRL

A.Fernández, A. Apituley, F.Molero, M.Pujadas, H.Russchenberg

Introduction and motivation

Upper tropospheric water vapour plays a key role on the global radiation budget (Mocker, 1995) so that, accomplishing reliable data at that altitude it is crucial to better understand it. However due to its low concentration and location this task remains a challenge.

Likewise, It is very well known that aerosols represent the largest single source of uncertainty in the total anthropogenic radiative forcing of the atmosphere, in particular concerning the influence of aerosol on cloud formation processes and cloud characteristics (Forster et al., 2007).

On another note, temperature is one the parameters that characterizes the thermodynamic state of the atmosphere and define other variables as relative humidity, which in turn, controls cloud formation and aerosol optical properties (Mattis et al., 2002).

Given the fact that multiwavelength Raman lidars have the potential to provide aerosol optical properties, water vapour mixing ratio and temperature profiles (depending on its configuration) with high resolution in time and vertical dimension, they represent a powerful tool to study these phenomena (Bösenberg et al., 2003). Additionally, when the previously mentioned configuration is implemented, multiwavelength Raman lidars are able to furnish relative humidity since this parameter can be estimated from a set of temperature, pressure and water vapour mixing ratio profiles. Temperature and water vapour mixing ratio profiles can be retrieved by the Raman lidar technique, however, an independent calibration source is needed.

Scientific objectives

According to the reasons outlined above, the initial proposed scientific objectives in ACIRL (Aerosol Cloud Interaction and Raman Lidar) are defined as follows:

1º To assess the stability and uncertainty of the water vapour calibration constant since Raman lidar measurements of specific humidity require an independent calibration source to provide trustworthy mixing ratio measurements.

2º To gain experience with the pure rotational Raman (PRR) lidar to derive temperature profiles while assistance with this experimental equipment. Cloud formation processes can be best described in terms of the relative humidity (Rh) rather than the specific humidity (Q). Temperature information is needed to convert Q to Rh. The pure rotational Raman lidar technique offers the possibility to measure the temperature profile simultaneously and in the same atmospheric volume as the water vapour profile.

3º To study simultaneous measurements of humidity conditions and aerosol optical properties, in particular, backscatter and extinction coefficients as well as backscatter-derived Angström exponents on different synoptic situations. Special interest will be focused on studying the uptake of water vapour by hygroscopic aerosols in cloudy conditions.

Reason for choosing the CESAR station:

1º Its long experience in lidar remote sensing, specially as regards aerosol and water vapour measurements.

2º Its wide range of ancillary instrumentation to support lidar data.

3º Its different meteorological conditions when compared to the Madrid lidar station. In particular, when low cloud formation takes place as this phenomenon is easily observed at CESAR station but it rarely occurs in Madrid.

4º The similarities with Madrid in the distance between the radiosondes and the lidar station.

Method and experimental set up

1º As an independent source of calibration is required to obtain trustworthy water vapour measurements, operational radiosondes are used for this purpose. The calibration has been performed by a linear fit between the two Raman channel ratio($H_2O_{(v)}$ - 407 nm and N_2 - 387 nm) and radiosounding mixing ratio measurements. This calibration has assumed no dependent term, so that, the slope has been forced to go through coordinates (0,0). The altitude range for calibration has been set at 3 km AGL and the calibrating layer has been 1 km thick. Although these parameters have been modified in certain cases when no agreement was found between lidar and tower mixing ratio observations. Since radiosondes are routinely launched at De Bilt, which is located at 25 km from CESAR station, some discrepancies can be expected due to spatial and time differences. Lidar mixing ratio uncertainty has been also estimated and it includes statistical errors plus standard deviation from the calibration procedure, although propagated errors associated to radiosounding have not been included yet. For this purpose the GRUAN RS92 data product will be used in the near future.

Following on from this point, the CESAR station has a 200 meter meteorogical tower, which has been used to compare water vapour measurements at 200 m from the Caeli lidar (Apituley et al., 2009). Lidar mixing ratios at 200 m have been calculated by averaging the mixing ratio in the range 150-250 m and so do its errors. The tower provides the mixing ratio. However no associated errors, therefore, the mixing ratio has been independently estimated by the following expression along with its errors (propagated errors).

$$r = 0.622 \cdot e/p - e \quad (1)$$

Where *r* stands for mixing ratio, *e* water vapour pressure and *p* pressure. As there is no available pressure data at 200 m AGL, pressure at this altitude has been extrapolated from ground level pressure data at a rate of -1hPa/8m. The water vapour pressure has been retrieved by the empirical approximation to the Clausius-Clapeyron equation along with its error (propagated error).

Finally, the comparison between lidar and tower mixing ratio observations has allowed us to assess the agreement between both measurements.

2º A number of 7 EARLINET observations were carried out (including special events as advected smoke from Canadian forest fires) under supervision of A. Apituley. These lidar performances have provided a technical training on Caeli lidar and also on multiwavelength Raman lidar techniques. Likewise, a substantial training has been received when processing lidar data, in particular concerning Raman signal by Ansmann algorithm. However, as a result of bad weather conditions, the experiments with the PRR temperature have been postponed.

On the other hand, It has been possible to assist the iSPEX (Spectropolarimeter for Planetary EXploration) campaign which has been a fruitful experience since it represents an innovative way to measure aerosols properties such as refractive index by means of iPhones. Its performance is based on measuring the intensity of the spectrum and the degree of polarization for visible light. Further information can be found at http://ispex.nl/en/.

3º A lidar database has been collected and 15 cases have been selected to be studied, mostly in variable cloud conditions. The criteria to select these cases is based on presence of nighttime conditions to better retrieve lidar products (water vapour mixing ratio, lidar ratio and extinction coefficient as Raman signals get affected by solar background) and also on presence of low clouds, in particular those located just on top of the boundary layer. Thus, there is a possibility to study and relate optical aerosol properties at near cloudy conditions to aerosols at ground level when these data are available. This relationship only must be established under a well mixed boundary layer and convective circulation inside of the boundary layer. Advected clouds must be discarded. Hence, it is necessary to study the meteorological situation in each case. Nonetheless this is a secondary aim to be fulfilled subsequently. The main aim is explained as follows.

For the previously mentioned cases, extinction and backscatter coefficient profiles have been retrieved by the Ansmann (1992) algorithm for wavelengths 355 and 532 nm as well as its lidar ratio. As initially implemented Ansmann algorithm in the software, backscattering resolution function was set at 100 and extinction resolution function at 300, both for the near range. Thus, the lidar ratio has been retrieved under these conditions (different resolution function for extinction and backscattering) for every single lidar case. Given the fact that lidar ratio represents the ratio of the extinction coefficient over backscattering coefficient, both variables should have the same resolution function so as to avoid spurious effects in lidar ratio. Therefore, backscattering and extinction profiles have been retrieved subsequently again using the same resolution function for both variables (extinction and backscattering) at values of 100, 150, 200 and 300 (it is required to find a proper trade-off between spatial/temporal resolution and noise, moreover, high resolution is needed close to cloud base). Though this sensitivity analysis has

been carried out for a few cases, preliminary results have lead us to conclude that using a resolution function of 100 is too high because it introduces a high noise in extinction profiles, and consequently to noisy lidar ratio profiles. When a resolution of 300 is used, noisy signals have not been found as a problem any longer, however smoothing is too high to identify accurate aerosol structure in the atmospheric column analyzed. In consequence, resolution function of 150 seems the best option in order to avoid noisy lidar ratio as well as to have enough resolution for lidar ratio. As a result, every lidar case has been studied by the Ansmann algorithm twice, firstly using different resolution function for backscattering and extinction (100 and 300 respectively) and secondly applying the same resolution function of 150 for backscattering and extinction. It is not clear yet which retrieval works best as different results have been found. After conversation with A. Apituley, it is concluded that it might be thought-provoking to study the retrieval when different resolution function has been implemented for backscattering and extinction and afterwards to proceed to backscattering integration and subsequently backscattering derivation using the same resolution function as extinction (as suggested after private conversation between A. Apituley and I.B. Serikov). This is work to be done in the near future.

Additionally, retrievals of backscattering and extinction coefficient profiles have been also carried by Klett-Fernald (Klett, 1981; Fernald, 1984) algorithm (assuming LR values of 20 and 50 sr) for wavelengths 355, 532 and 1064 nm so as to be compared with the two previous Ansmann retrieval. Backscatter-derived Angström exponents have been estimated too for every retrieval (Ansmann and Klett algorithm). Backscattering and extinction coefficient errors have been also estimated and so do its derived products (backscatter-derived Angström exponents and lidar ratio) although just the lidar ratio error and extinction coefficients will be shown.

Furthermore, relative humidity has been determined from the mixing ratio lidar measurements along with pressure and dew point data obtained by radiosondes. It involves the assumption of pressure and temperature profiles for the CESAR station equal to the radiosonde launch site. Thence lidar and radiosondes relative humidity profiles have been depicted to be compared.

Finally, another few cases have been also selected to be compared as they represent clear sky conditions or unusual type of aerosol for the Netherlands (for instance saharan intrusion).

Preliminary results and conclusions

1º Water vapour channel calibration.

Table 1 and Figure 1 depict measurements used in the calibration process as well as calibration constant variability.

Number of observations	Date	Time
1	28/03/2011	18:30-19:30
2	07/04/2011	18:40-19:40
3	18/04/2011	19:00-20:00
4	02/05/2011	20:00-21:10
5	09/05/2011	19:30-21:10
6	30/05/2011	16:30-18:30
7	02/06/2011	20:20-21:40
8	27/06/2011	19:30-22:00
9	30/06/2011	19:30-22:00
10	04/07/2011	19:00-21:30
11	01/08/2011	19:00-21:10
12	15/08/2011	18:10-21:00
13	16/01/2012	18:40-20:20
14	02/02/2012	18:20-20:20
15	06/02/2012	18:00-19:30
16	20/02/2012	18:30-20:40
17	19/03/2012	20:00-22:00
18	22/03/2012	19:30-21:40
19	26/03/2012	19:50-21:00
20	21/05/2012	20:20-21:00
21	24/05/2012	20:20-21:30
22	18/04/2013	20:00-20:30

Table 1. Lidar measurements.

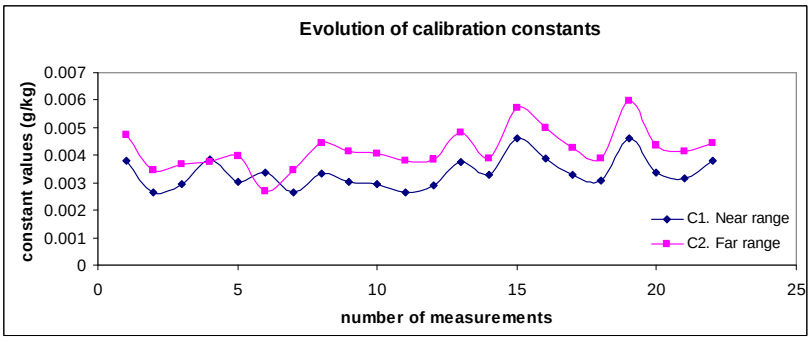

Figure 1. Evolution of calibration constants.

As two different telescopes (near range and far range) are available for Caeli lidar, two calibration constants have been calculated for every measurement. The calibration constant average for the near range (C1) is 0,0034 g/kg with standard deviation of 0.00056 g/kg which represents approximately 17% of variability. The calibration constant average for the far range (C2) is 0,0042 g/kg with standard deviation of 0.00073 g/kg which represents approximately 17.5% of variability.

There are several reasons which might explained this variability. Firstly, it might be associated to alignment processes carried out in every single measurement. Secondly, It might be due to a suboptimal altitude range in the calibration processes. Finally, differences between both measurement sites in terms of time and space might also be responsible for this variability. Therefore, further research is necessary so as to better understand this variability. Nonetheless,

once calibration was performed, mixing ratio lidar measurements agreed well with water vapour mixing ratio obtained by the meteorological tower at 200 meter agl as it is shown in Figure 2 and 3.

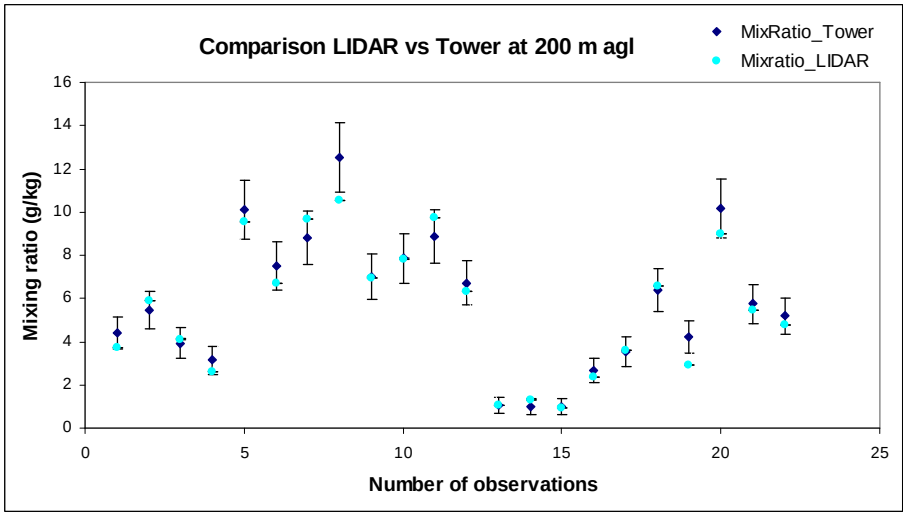

Figure 2. Mixing ratio measurements obtained by lidar and tower at 200 m agl.

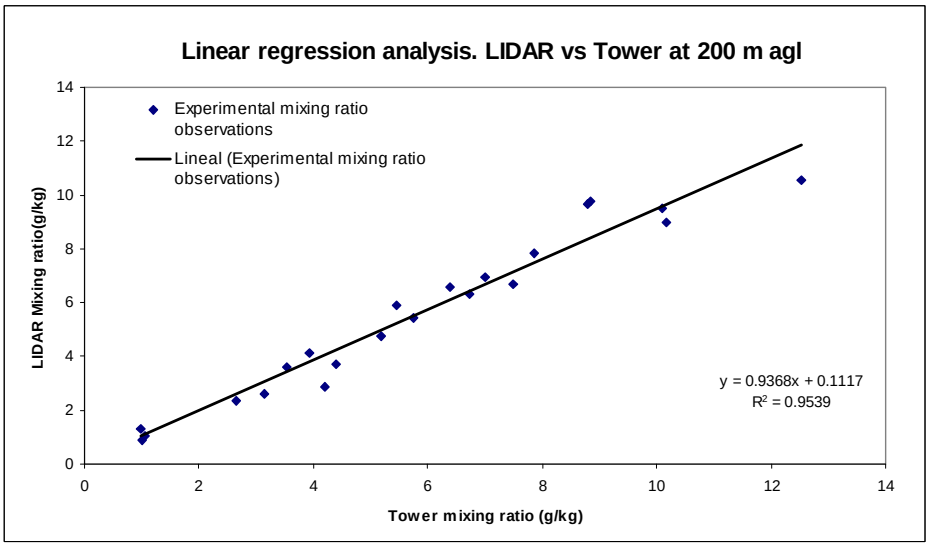

Figure 3. Linear regression analysis between lidar and tower mixing ratio observations at 200 m agl.

These results are not trivial, since most lidar have an incomplete overlap at close range which means overlap function is cancelled and optical path for nitrogen and water vapour raman signal must be equal. Besides, spatial and time differences between both measuring location seem not to be significant.

As regards error bars in figure 2, lidar mixing ratio errors are lower than expected (error bars are almost not noticeable) and it is probably caused by not including the propagated error from radiosounding in the total error estimation. Further work must be done to include this term so as to perfectly characterize the lidar mixing ratio error. Concerning the linear regression analysis, a clear agreement between these two observations is reached. These preliminary results confirm that radiosondes are a reliable external source for water vapour lidar calibration even though radiosonde launch site is located 25 km away from CESAR but also it proves that tower mixing ratio observations at 200 m agl might be used as an external source of calibration for Caeli.

3º Study cases.

As detailed below in table 2, 15 study cases have been analyzed under the same procedure but only just one case is commented here. Further analysis of these cases will be carried out by available ancillary measurements, in particular by HTDMA for the year 2008.

Date (DD/MM/YYYY)	Time (UTC)
11/05/2008	12:07-12:15
12/05/2008	23:23-00:00
19/05/2008	11:55-12:05
19/05/2008	20:00-20:30
20/05/2008	22:00-0:00
21/05/2008	10:27-10:35
22/05/2008	6:00-6:30
01/02/2010	16:49-16:57
07/04/2011	18:50-18:55
18/04/2011	18:56-20:00
02/05/2011	19:59-21:13
09/05/2011	19:31-21:10
23/05/2011	22:00-22:10
27/06/2011	19:28-22:00
20/02/2012	17:33-17:38

Table 2. Date and time of lidar observations for cloud-aerosol-humidity interactions.

Cloudy case

The following lidar case has been analyzed for the time period ranged between 23:23 and 0:00 on 12 May 2008. As it can be noticed in quicklooks (Figure 4 and 5) cloud formation is taking place on the top of the boundary layer at 3 km high. Although the layer where clouds are situated presents high variability in terms of the range corrected signal (due to the cloud nature), the whole period of the lidar measurement has been processed since atmospheric layers below clouds remain constant and stratified.

Looking at figures 6 and 7, lidar and radiosonde relative humidity observations (HR_LIDAR and HR_rs respectively) have been depicted, proving no significant discrepancies. Along with it, the lidar ratio at 355 nm and its error have been illustrated. The lidar ratio at 355 nm has been estimated from backscattering and extinction coefficients retrieval under initial different resolution functions (LR355. AA_IR) in figure 6. Likewise, the lidar ratio at 355 nm has been estimated from backscattering and extinction coefficients retrieval under the same resolution function of 150 (LR355. AA_SR). As previously commented it is complex to determine which retrieval works better since the same resolution function for backscattering and extinction provides a noisier lidar ratio value, however the different resolution function for backscattering and extinction might be overestimating the lidar ratio at different levels. Anyhow, what is really noticeable is a positive correlation found between relative humidity and the lidar ratio at 355 nm (the lidar ratio at 532 nm is not shown as the Raman signal at this wavelength is often too noisy to be processed reliably) in both figures (6 and 7). When the water vapour uptake by aerosols takes place, changes in their optical properties are induced. This leads to a rapid increase in their extinction coefficient when compared to backscattering coefficient, and therefore and increase in their lidar ratio. This positive correlation between lidar ratio and relative humidity was expected as previous works have already shown relationships between extinction coefficient and humidity (Zieger et al., 2011). Nonetheless, once the water vapour starts to condense on the aerosol surface and cloud formation starts, a significant increase in backscattering coefficient is identified, leading to a sudden decrease in lidar ratio. As represented in such figures, an increase in lidar ratio at 355 nm (from 20 to 60 sr) is produced and at the same time relative humidity profiles evolves from 40 to 90 % in the altitude range established between 1000 to 2650 meters AGL. From this altitude on, near saturation conditions are reached and cloud formation starts as it is noticed by sharp decrease in lidar ratio at this altitude.

On the other hand, the extinction coefficient profiles at 355 nm (in Fig. 8) have approximately doubled its value in the altitude range 1000-2650 m AGL (relative humidity values evolve from 40 to 90%) which partially might be due to water vapour uptake. Finally, concerning the Angström exponents, the Ansmann algorithm retrieval at 532 and 355 have confirmed that it is the best source to estimate this parameter as can be noticed in Figure 10. Having a look at AE 532-355.AA_SR and AE 532-355. AA_IR in Figure 10 (blue and pink line), it is identified a significant decrease in Angström exponent for the altitude range 2500-2650 m, which points out a sudden aerosol growth very likely due to water uptake as relative humidity is about 90 %. This case is not analyzed beyond 2650 m high as cloud formation has already taken place and optical aerosol properties retrieval become tricky. Further analysis will be done for the 15 selected cases, although preliminary results have shown that water vapour uptake may be identified using the lidar ratio and Angström exponents.

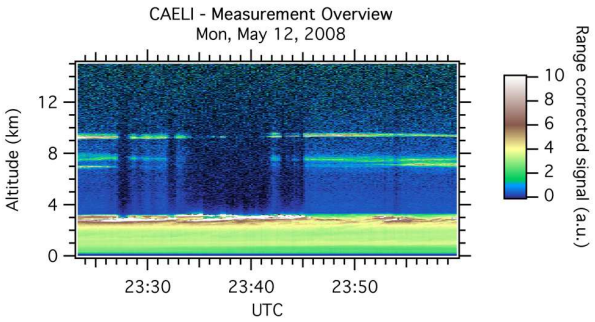

Fig. 4. Far range corrected signal at 1064 nm.

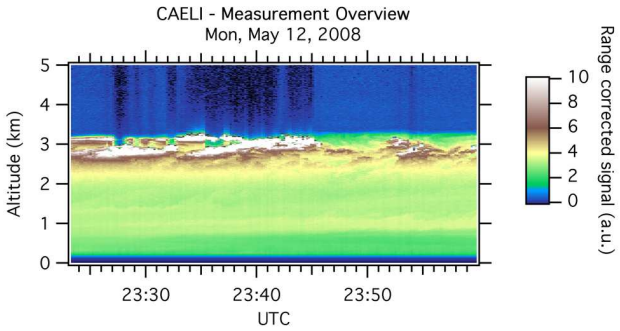

Fig. 5. Near range corrected signal at 1064 nm.

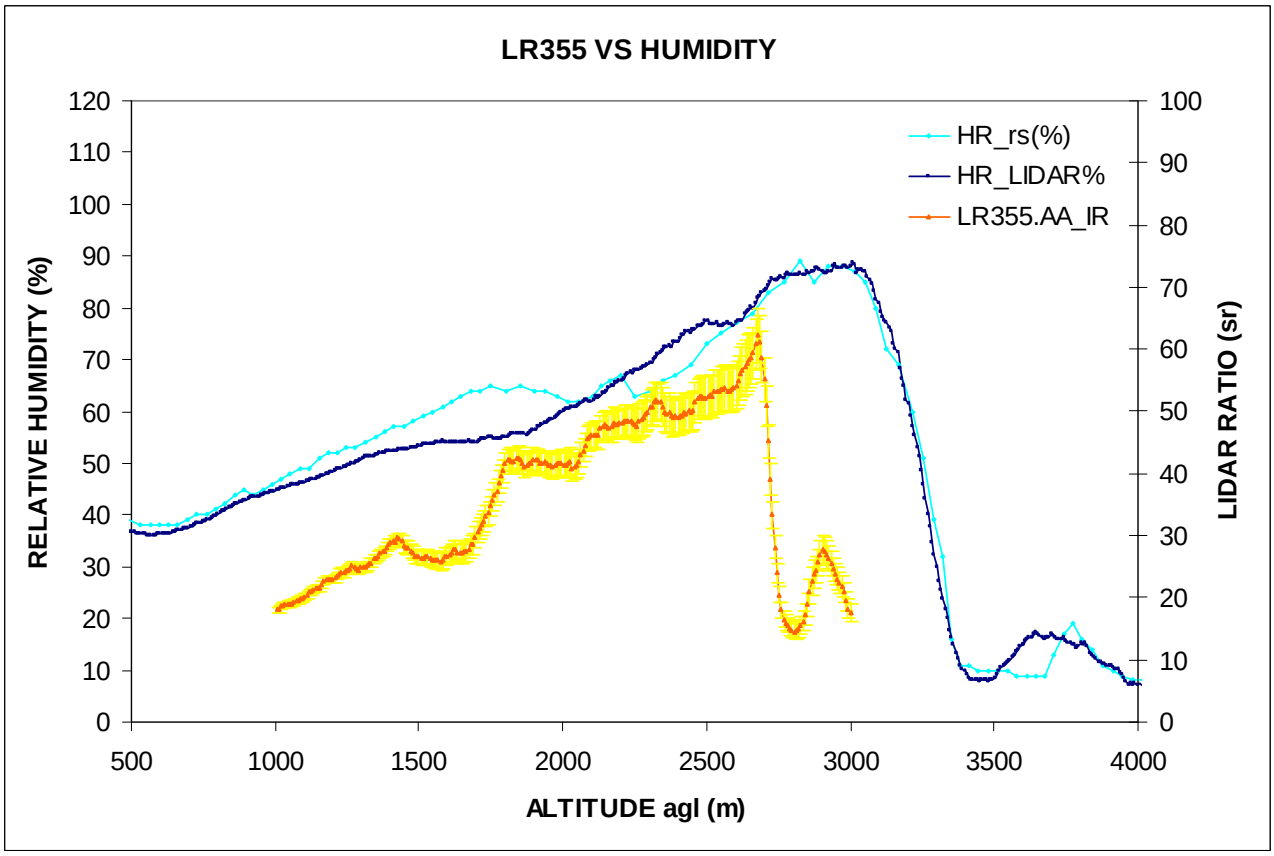

Figure 6. Profiles of lidar ratio at 355 nm ((IR) Different resolution function for backscattering and extinction) and relative humidity estimated by lidar and radiosounding.

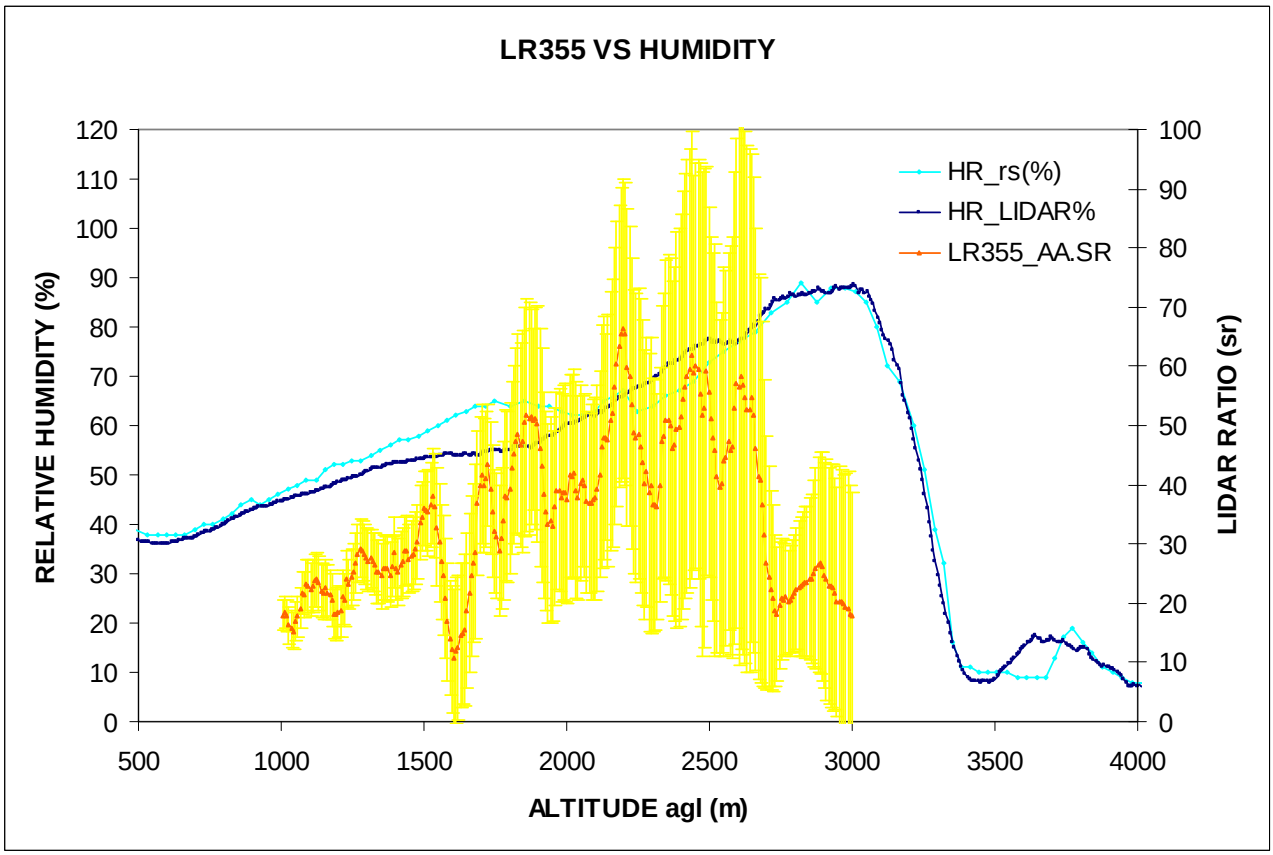

Figure 7. Profiles of the lidar ratio at 355 nm ((SR) same resolution function for backscattering and extinction) and relative humidity estimated by lidar and radiosounding.

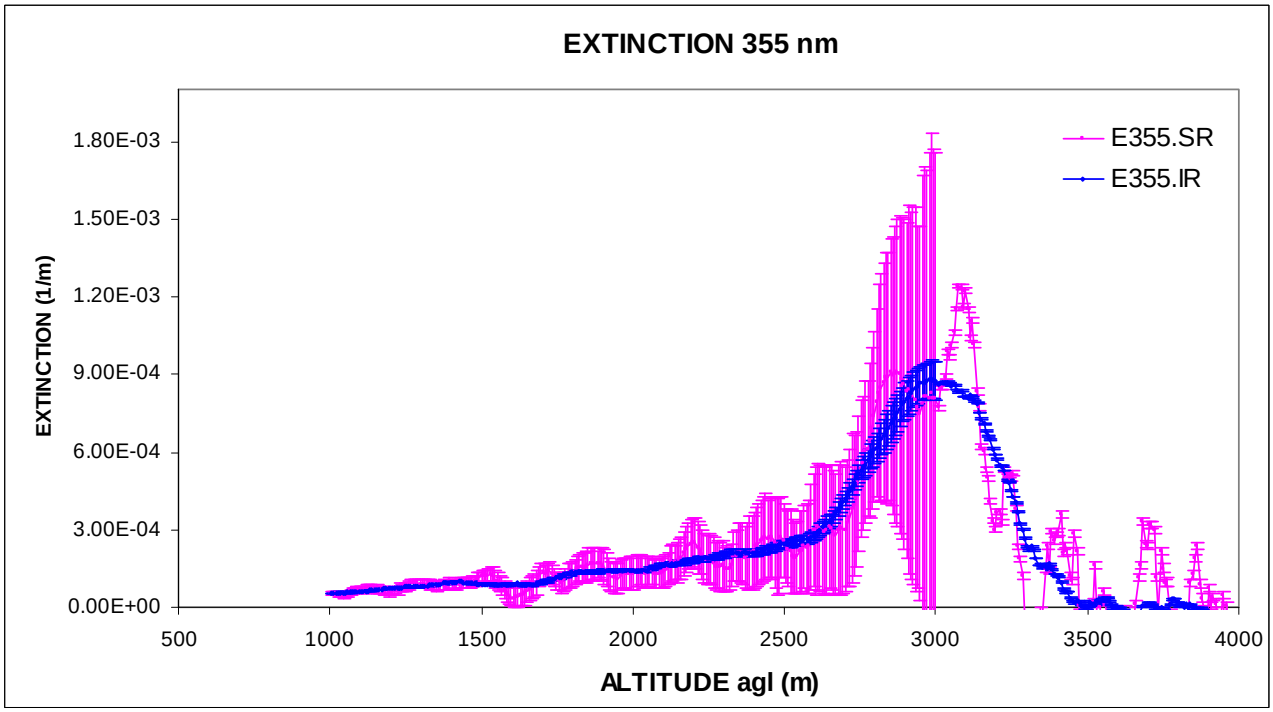

Figure 8. Profiles of the extinction coefficient at 355 nm (IR=Resolution function of 300, SR = Resolution function of 150) and its errors.

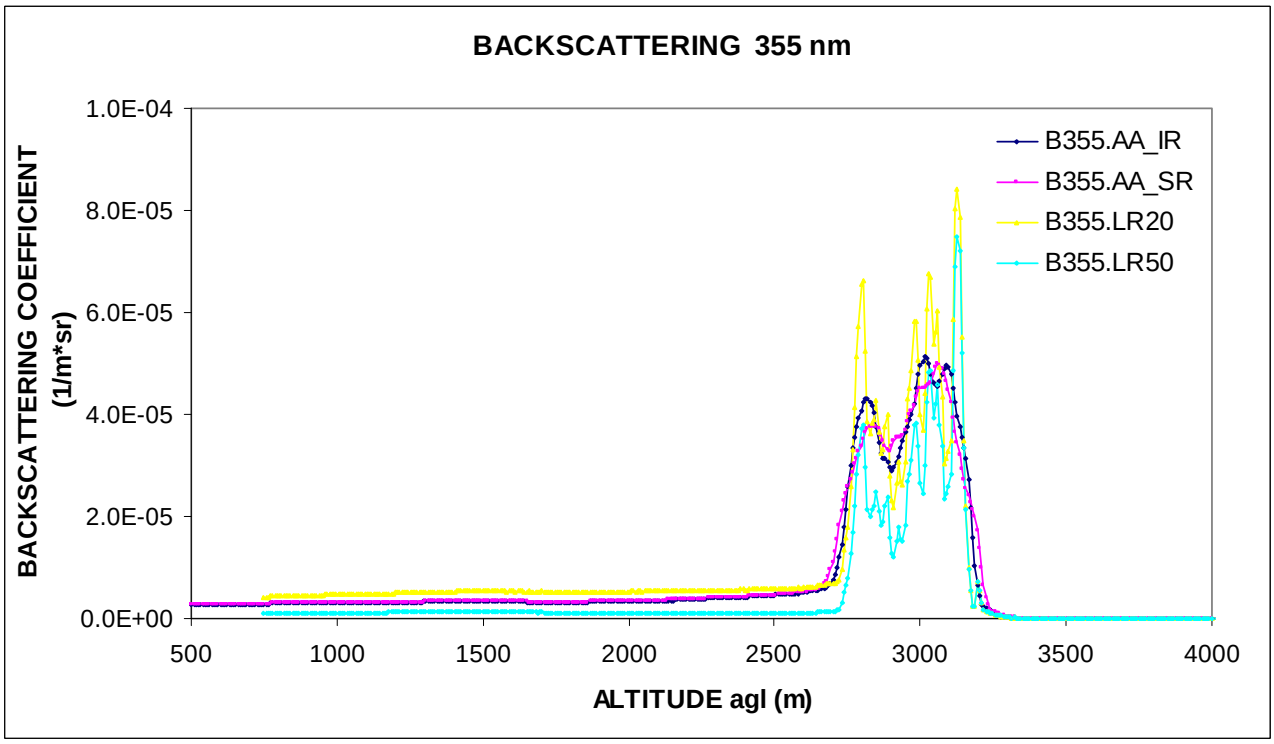

Figure 8. Profiles of the backscattering coefficient at 355 nm by the Klett-Fernald (asumming lidar ratio values of 20 and 50) and the Ansmann algorithm ((SR) same resolution function for backscattering and extinction. (IR) Different resolution function for backscattering and extinction).

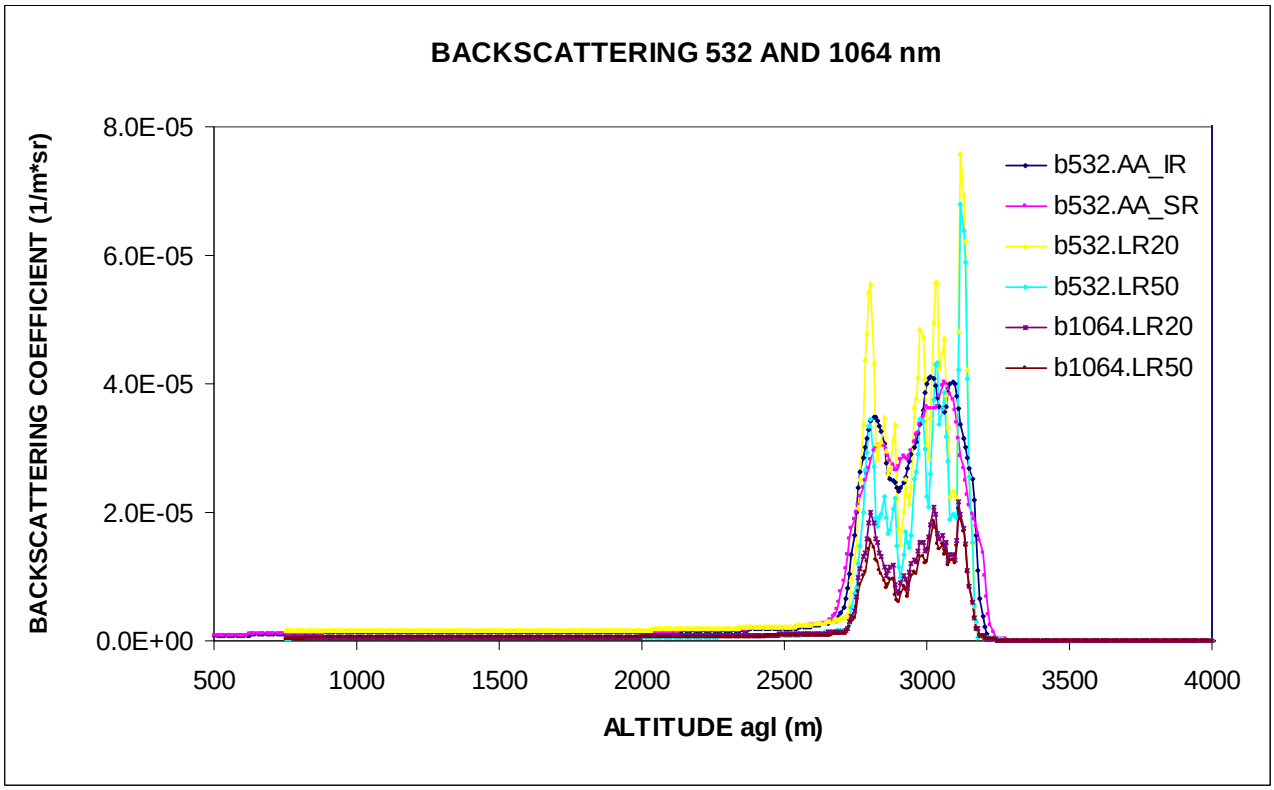

Figure 9. Profiles of the backscattering coefficient at 532 and 1064 nm by the Klett-Fernald (asumming lidar ratio values of 20 and 50) and backscattering coefficient at 532 nm by the Ansmann algorithm ((SR) same resolution function for backscattering and extinction. (IR) Different resolution function for backscattering and extinction).

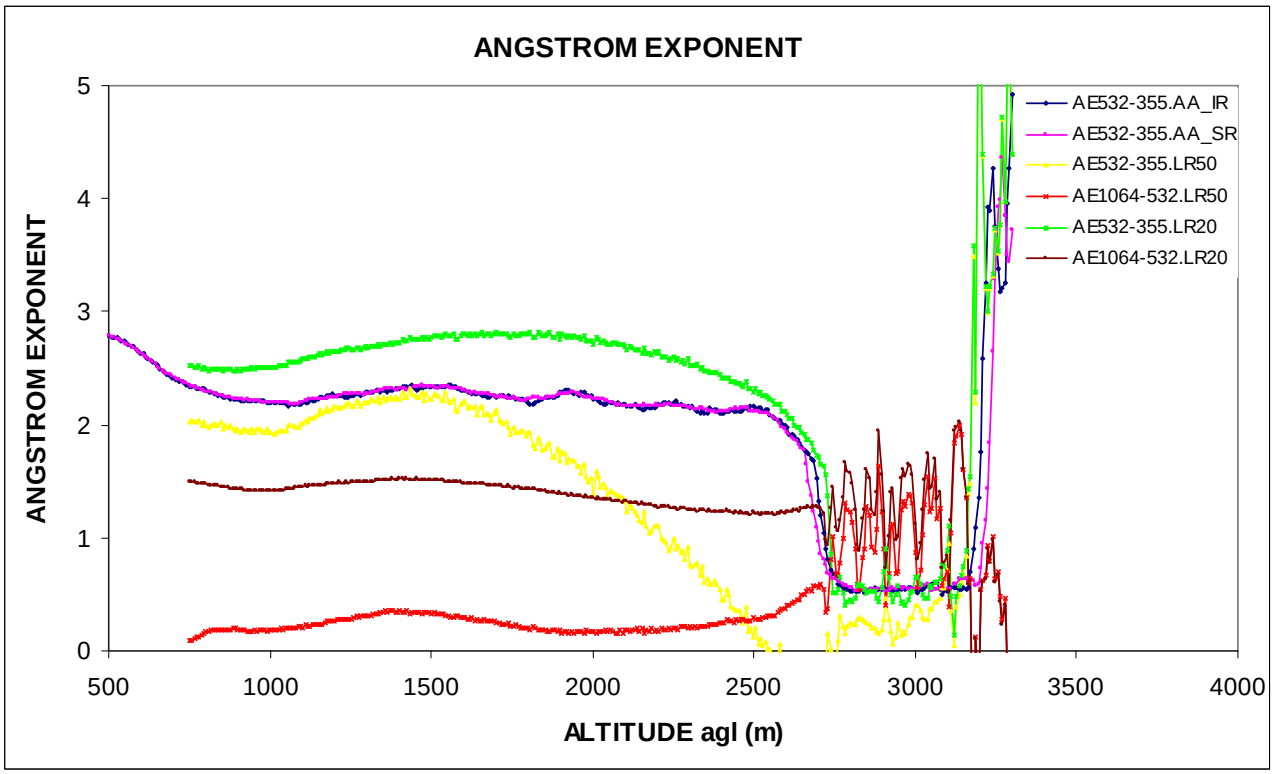

Figure 10. Profiles of the backscatter-derived angström exponents from previous backscattering coefficient retrievals.

Outcome and future studies

As commented, further analysis will be carried out on such derived-lidar products for 15 selected cases. What is more, aerosols at ground level will be studied in correlation with HTDMA database for selected cases to better study the water vapour uptake phenomenon. Additionally, the boundary layer will also be studied by parameters as potential virtual temperature and other indices of turbulence as the Richardson number which will supply more information about the mixing grade of the atmospheric boundary layer. Synoptic situations and backward trajectories will also be taken into account. These result might lead to better characterize aerosol inside of boundary layer and relate them to low clouds.

Comments

During the two months period stay an interesting interaction with K. Sarna (Ph. D. student at TU-Delft) has also been established as she also works on cloud-aerosol interaction framework (ACTRIS WP22).

References

Ansmann, A., U. Wandinger, M. Riebesell, C. Weitkamp, W. Michaelis, "Independent measurement of extinction and backscatter profiles in cirrus clouds by using a combined Raman elastic-backscatter lidar," *Appl. Opt*., vol. 31, pp. 7113-7131, Nov. 1992.

Apituley, A., K. M. Wilson, C. Potma, H. Volten and M. de Graaf, "Performance Assessment and Application of Caeli - A high performance Raman lidar for diurnal profiling of Water Vapour, Aerosols and Clouds". Presentation: 8th International Symposium on Tropospheric Profiling, 19/10/2009-23/10/2009, A. Apituley, H. W. J. Russchenberg, W. A. A. Monna (Ed), Proceeding of the 8th International Symposium on Tropospheric Profiling, ISBN 978-90-6960-233-2. Delft, 2009.

Bösenberg, J., V. Matthias, A. Amodeo, V. Amoiridis, A. Ansmann, J. M. Baldasano, I. Balin, D. Balis, C. Böckmann, A. Boselli, G. Carlsson, A. Chaikovsky, G. Chourdakis, A. Comerón, F. De Tomasi, R. Eixmann, V. Freudenthaler, H. Giehl, I. Grigorov, A. Hågård, M. Iarlori, A. Kirsche, G. Kolarov, L. Komguem, S. Kreipl, W. Kumpf, G. Larchevˆeque, H. Linné, R. Matthey, I. Mattis, A. Mekler, I. Mironova, V. Mitev, L. Mona, D. Müller, S. Music, S. Nickovic, M. Pandolfi, A. Papayannis, G. Pappalardo, J. Pelon, C. Pérez, R. M. Perrone, R. Persson, D. P. Resendes, V. Rizi, F. Rocadenbosch,. A. Rodrigues, L. Sauvage, L. Schneidenbach, R. Schumacher, V. Shcherbakov, V. Simeonov, P. Sobolewski, N. Spinelli, I. Stachlewska, D. Stoyanov, T. Trickl, G. Tsaknakis, G. Vaughan, U. Wandinger, X. Wang, M.Wiegner, M. Zavrtanik, C.

Zerefos, “EARLINET: A European Aerosol Research Lidar Network to establish an aerosol climatology”, Rep. 348, Max-Planck Inst. für Meteorol., Hamburg, Germany (2003).

Fernald, F., G. “Analysis of atmospheric lidar observations: some comments”, *Appl. Opt*., 23, 652-653, 1984.

Forster, P., V. Ramaswamy, P. Artaxo, T. Berntsen, R. Betts, D. W. Fahey, J. Haywood, J. Lean, D. C. Lowe, G. Myhre, J. Nganga, R. Prinn, G. Raga, M. Schulz, R. Van Dorland., “Changes in atmospheric constituents and in radiative forcing”, in Climate Change 2007: The Physical Science Basis, Contribution of Working Group I to the Fourth Assessment Report of IPCC, S. Solomon Edt., pp. 129–234, Cambridge Univ. Press, U.K. (2007).

Klett J. D. “Stable analytic inversion solution for processing Lidar returns”, *Appl. Opt*., 20, 211-220, 1981.

Mattis, I., A. Ansmann, D. Althangen, V. Jaenisch, U. Wadinger, D. Müller, Y. F. Arshinov, S. M. Bobrovnikov, and I. B. Serikov. " Relative-humidity profiling in the troposphere with a Raman lidar", *Appl.Opt*., vol. 41, 6451-6462. 2002.

Mocker, S. B., “Water vapor in the climate system”, *Special report, American geophysical Union (AGU)*, 2000 Florida Ave., N.W., Washington, DC 20009, ISBN 0-87590-865-9, 1995 (http://www.eso.org/gen-fac/pubs/astclim/espas/pwv/mockler.html)

Zieger, P., E. Weingartner, J. Henzing, M. Moerman, G. de Leeuw, J. Mikkilä, M. Ehn, T. Petäjä, K. Clémer, M. van Roozendael, S. Yilmaz6, U. Frieß, H. Irie, T. Wagner, R. Shaiganfar, S. Beirle, A. Apituley, K. Wilson, and U. Baltensperger. " Comparison of ambient aerosol extinction coefficients obtained from in-situ, MAX-DOAS and LIDAR measurements at Cabauw*". Atmos. Chem. Phys*., 11, 2603–2624, 2011.